Transition modelling for flow separation in low-pressure turbine cascades

Geetam Saha[1], Rajesh Ranjan[2]

[1]Department of Construction Engineering, Jadavpur University, Kolkata, West Bengal 700032, India
[2]Department of Aerospace Engineering, Indian Institute of Technology Kanpur, Uttar Pradesh 208016, India

ABSTRACT

Low-pressure turbine (LPT) blades at high altitude present complex flow situations due to presence of separation and subsequent transition. These relatively low Reynolds number flows are challenging to simulate in a computationally affordable framework. Present work addresses this issue by providing solutions of such LPT flows using Reynolds-averaged Navier-Stokes (RANS) simulations. The simulations are performed on a cascade with Pratt & Whitney blade T106A. Simulation conditions are based on the experiments carried out at a transitional Re = 51,831 at a relatively high angle of incidence of 45.5°. Simulations were performed using several turbulence and transitional models. The computed results are compared with the experimental data as well as available Direct Numerical Simulation (DNS) results. All three turbulence models used for the study- Spalart-Allmaras (SA), k-ω SST and Realizable k-ϵ - predict the flow well on the pressure side of the blade but fail to capture the flow on the suction side due to involvement of separation and transition. However, when these simulations are performed with transition models (γ-Re_θ and the laminar kinetic energy (LKE)) on the same grid, significant improvements were seen in the prediction of the separation region. Both the models predicted the pressure plateau near the trailing edge of the suction side related to the separation region. A detailed flow analysis, further, suggests that compared to the γ-Re_θ model, the LKE model reproduces the separation bubble structure more accurately, close to that obtained from high-resolution direct numerical simulations in the literature.

Keywords: Low-pressure turbine, Flow separation, Separation-induced transition, Transition models

1. INTRODUCTION

Gas turbines consume around 95 billion gallons of aviation fuel globally [1]. Therefore, efficient design of gas turbines is of utmost importance in this regard as it will not only reduce the specific fuel consumption (SFC) along with savings of millions of dollars but will also help with a reduced environmental footprint.

Low-pressure turbine (LPT) is one of the most crucial components in a gas turbine. Statistics reveal that increase in efficiency of a LPT by 1% can result in reduction of SFC by 0.6 to 0.8% [2]. To obtain optimum efficiency, in depth understanding of physics of flow past turbine blades is essential.

However, it remains a challenging problem, both from experimental and computational perspectives, because of its complex nature of flows [3]. Specifically, the task of designing blades of a LPT is arduous because of the wide distinction in flow physics during different phases of flight such as the take off and cruise.

During cruise, the turbine inlet Reynolds number is appreciably less, up to a factor by 5, than the sea take off conditions [4]. This results in a change of flow regime from turbulent to laminar or transitional. A consequence of this is the escalation of stagnation pressure loss. Because of the design of LPT, a certain combination of flow conditions may lead to favorable pressure gradients up to mid chord of the blade at the suction side. Whereas on the latter half of the blade adverse pressure gradient is witnessed [5]. During cruise conditions at low isentropic exit Reynolds number, the laminar boundary layer may undergo a separation-induced transition leading to formation of turbulent wakes at aft portion of the blade at the suction side [6]. This transition is periodic unsteady due to incoming wakes from upstream blade rows [7].

The contact of the separated layer with free stream may favor Kelvin-Helmholtz (KH) instability. This results in quick transition and flow reattaches. This is commonly referred to as 'closed separation bubble' [8]. The size and length of separation bubble affects the overall blade losses [9]. Because of these reasons, there have been several efforts in the past to accurately predict these bubbles.

Unfortunately, not much experimental data for such flows are available in open literature and those which are available typically lack detailed description of the flow structure. Skoda *et al.* [10] made an effort to study the flow in a LPT cascade with several turbulence models under undisturbed and periodically disturbed flow. Through the comprehensive study, authors recommended determination of inflow conditions more accurately through further experimentation so that proper turbulent inflow conditions can be adopted in the numerical simulations. Nevertheless, a few experiment measurements [11,12] on these LPTs, both in on- and off-design conditions, clearly show a plateau in the wall pressure profile strongly indicating the presence of a flow separation region. Based on these experiments, there have also been several computational efforts to reproduce reliable flow physics. Kalitzin *et al.* [13] investigated the turbulent kinetic energy generated in a LPT cascade with great detail. The objective of the DNS was to

generate a database for validation and development of RANS turbulence models.

Ranjan et al. [14] in a high-resolution study on LPT found the deficient ability of classical boundary layer theory. The classical theory was able to deal with the effects of blade surface curvature. Zhao et al. [15] developed RANS models based on CFD driven machine learning framework. The novel model was utilized to model wake mixing in LPT and HPT. The high-resolution study by Ranjan et al.[14] emphasized upon the high sensitivity of bulk parameters like pressure distribution to grid resolution in case of flow past turbine blades [16]. Pichler et al. [17] highlighted upon the accuracy of RANS models in terms of prediction of flow through LPT. Ranjan et al. [18] presented a hybrid RANS solution which is computationally affordable for prediction of transitional flows.

However, most computational efforts which reasonably reproduced the real flow physics are unsteady simulations (Direct Numerical Simulation (DNS), Large Eddy Simulation (LES) etc.) involving very large number of grid points. These simulations are not affordable for engineering design and optimization of LPT blade. Therefore, in this work, we explore methodologies within Reynolds-averaged Navier-Stokes (RANS) framework that can produce reasonably accurate solution with prediction of separation and transition but without involving an inordinate grid size. The widely explored Pratt & Whitney high-lift blade T106A, for which experimental data is available [19], is used for the current study. These studies conducted at low Reynolds numbers and different inlet conditions present challenges for RANS simulations because of the presence of separation and transition. Therefore, simulations are performed with several turbulence and transitional models, and a comparative analysis is presented.

2. SPECIFICATION OF TEST CASE

Figure 1 shows the T106A turbine blade considered in the present study. The simulations are performed in a cascade at

high incidence based on experiments by Stadmuller [19] obtained in a low-pressure linear turbine test rig. In order to consider the flow as statistically two dimensional at midspan, seven aft loaded blades with an aspect ratio of 1.76 were tested [20]. The pitch to chord ratio was 0.799. Stagger angle of the blade under investigation was 30.7^0. In the original experiment the inlet flow angle was reported as 37.7^0. Upon numerical investigation of the same blade through high fidelity simulations like DNS and LES, uncertainty in the original inlet conditions were explained. inlet angle of 45.5^0 was suggested by Michelassi et al. [21].This angle has been used for the current study. The flow conditions (Re = 51,831 based on inlet velocity and axial chord length of the blade) are the same as used in the present work as per the experimental report of Stadtmuller [19].

3. METHODOLOGY

RANS (Reynolds Averaged Navier-Stokes) simulations were performed in the present study using the widely used commercial code ANSYS® Fluent® 20.1. The grid and boundary conditions used for the current work are shown in Figs. 1 and 2 respectively.
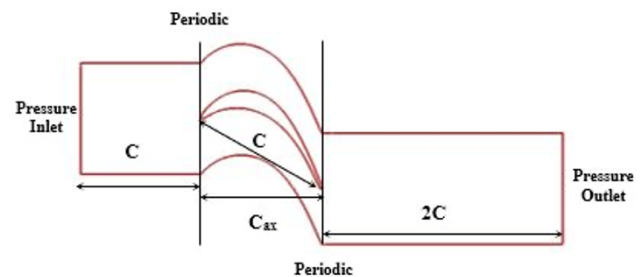
Figure 1: Computational Domain
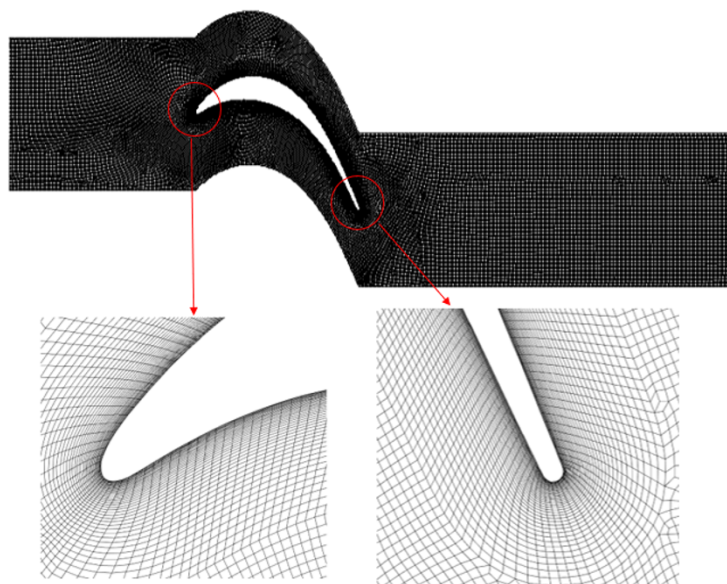
Figure 2: Finite Element Discretization of the 2D domain

Table 1: Flow Specification

Parameter	Value
Inlet flow angle (β_1)	45.5°
Total temperature at inlet (T_{t1})	312.9 K
Static pressure at inlet (p_1)	7,340 Pa
Total pressure at inlet (p_{t1})	7,770 Pa
Static pressure at exit (p_2)	6,950 Pa

Periodic boundary conditions are imposed in pitch-wise direction. The inflow boundary is located at one chord (C) upstream of the leading edge. Outflow boundary is located at $2C$ downstream of the trailing edge. C_{ax} represents the axial chord length of the blade in Figure 1.

The grid size used for RANS simulations consists of 63551 unstructured elements. A fine boundary layer mesh was created around the blade. 40 layers with the first cell height less than $Y^+ < 1$ (shown later). A growth rate of 1.075 was chosen for the boundary layer mesh. All quad elements were used for meshing of the entire domain.

All the simulations were performed in two-dimension (2D) for steady inflow with no upstream wake. The flow on the blade is solved using pressure-based solver available in FLUENT as the Mach number of the is quite low. Free stream turbulence intensity of 2% was utilized. Blade surface was specified with isothermal free no-slip boundary condition. The inlet and outlet boundary conditions were specified as per the details presented in Table 1.

For prediction of flow in gas turbines, RANS based solvers are used widely. RANS are cheaper alternatives to DNS and LES but they do not resolve any turbulent fluctuations, but rather model them. This reduced accuracy is a result of the Boussinesq approximation for stress strain relationship [22,23].

In the present work, three commonly used turbulence models are used. They are Spalart-Allmaras (SA) model, k-ω SST model, Realizable k-ϵ model. The descriptions of these models are available in [24]. Apart from these turbulence models, two models are used which have the ability to capture transitional flow. First is the γ-Re$_θ$ model. In the current solver, this model is implemented as a four-equation model: turbulence kinetic energy (Eq. 1) and specific dissipation rate equations (Eq. 2) of kω-SST model, and two more transport equations for capturing transition: intermittency (γ) (Eq. 3) and momentum thickness Reynolds number (Re$_θ$) (Eq. 4).

$$\frac{\partial(\rho k)}{\partial t} + \frac{\partial(\rho u_j k)}{\partial x_j} = P_{ta} - \beta^*\rho\omega k + \frac{\partial}{\partial x_j}\left(\left(\mu + \sigma_k\mu_t\right)\frac{\partial k}{\partial x_j}\right) \quad (1)$$

$$\frac{\partial(\rho\omega)}{\partial t} + \frac{\partial\left(\rho u_j \omega\right)}{\partial x_j} = \frac{\gamma}{\nu_t}P_{ta} - \beta\rho\omega^2 +$$
$$\frac{\partial}{\partial x_j}\left(\left(\mu + \sigma_\omega\mu_t\right)\frac{\partial\omega}{\partial x_j}\right) + 2(1-F_1)\frac{\rho\sigma_{\omega2}}{\omega}\frac{\partial k}{\partial x_j}\frac{\partial\omega}{\partial x_j} \quad (2)$$

$$\frac{D(\rho\gamma)}{Dt} = P_{\gamma1} - E_{\gamma1} + P_{\gamma2} - \frac{\partial}{\partial x_j}\left[\left(\mu + \frac{\mu_t}{\sigma_f}\right)\frac{\partial\gamma}{\partial x_j}\right] \quad (3)$$

$$\frac{D(\rho re_\theta)}{Dt} = P_{\theta t} + \frac{\partial}{\partial x_j}\left[\sigma_\theta(\mu + \mu_t)\frac{\partial Re_\theta}{\partial x_j}\right] \quad (4)$$

The second model is laminar kinetic energy (LKE) model or 'Transition k-kl-ω' model. This model employs three transport equations for turbulent and laminar kinetic energies and specific dissipation rate (Eqs. 5 to 7). These are based on the framework of k-ω model.

$$\frac{D(\rho k)}{Dt} = \rho(P_k + R_{BP} + R_{NAT} - \omega k - D_T) + \frac{\partial}{\partial x_j}\left(\left(\mu + \frac{\rho\alpha_T}{\sigma_k}\right)\frac{\partial k}{\partial x_j}\right) \quad (5)$$

$$\frac{D(\rho K_L)}{Dt} = \rho\left(P_{k_L} - R_{BP} - R_{NAT} - D_L\right) + \frac{\partial}{\partial x_j}\left(\mu\frac{\partial k_L}{\partial x_j}\right) \quad (6)$$

$$\frac{D(\rho\omega)}{Dt} = \rho\left(C_{\omega1}\frac{\omega}{k}P_k + \left(\frac{C_{\omega R}}{f_W}-1\right)\frac{\omega}{k}(R_{BP}+R_{NAT}) - C_{\omega2}\omega^2 + C_{\omega3}f_\omega\alpha_T f_W^2\frac{\sqrt{k}}{d^3}\right) + \frac{\partial}{\partial x_j}\left(\left(\mu + \frac{\rho\alpha_T}{\sigma_\omega}\right)\frac{\partial\omega}{\partial x_j}\right) \quad (7)$$

4. RESULTS & DISCUSSION
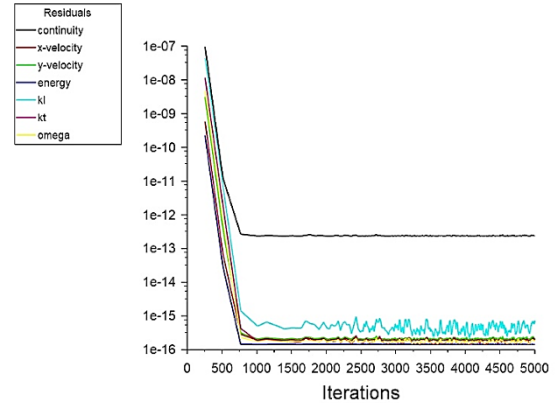
Figure 3: Residuals: LKE Model
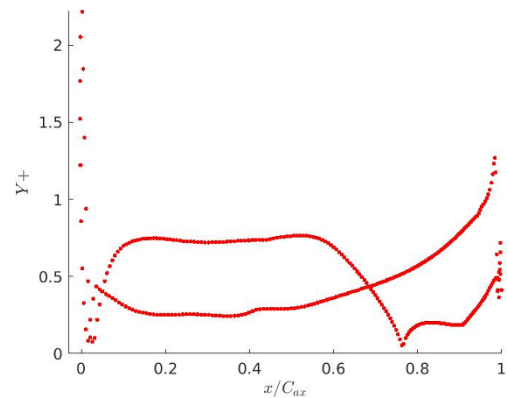
Figure 4: First-layer distance in wall-units
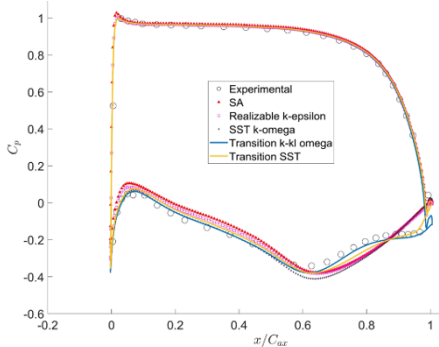
Figure 5: Pressure Coefficient
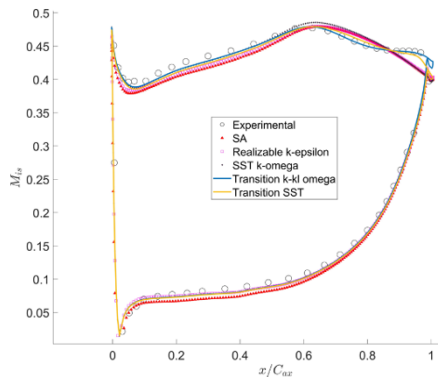
Figure 6: Isentropic Mach Number
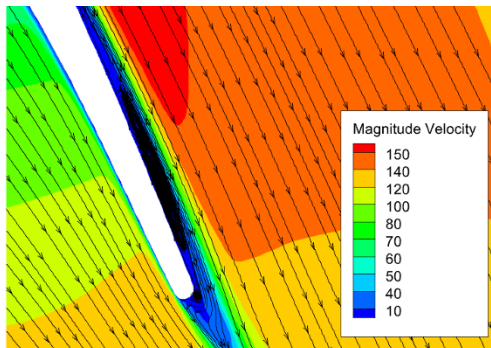
Figure 7: Velocity Streamlines (γ-Re_θ)
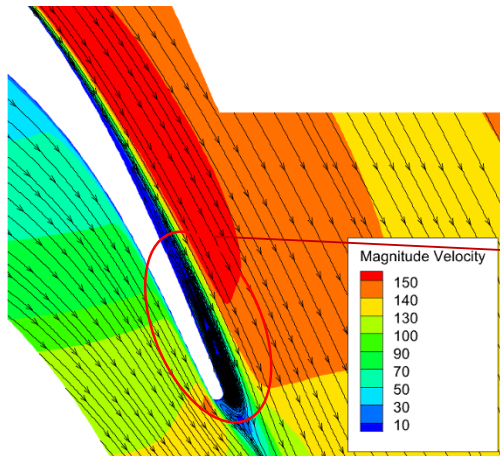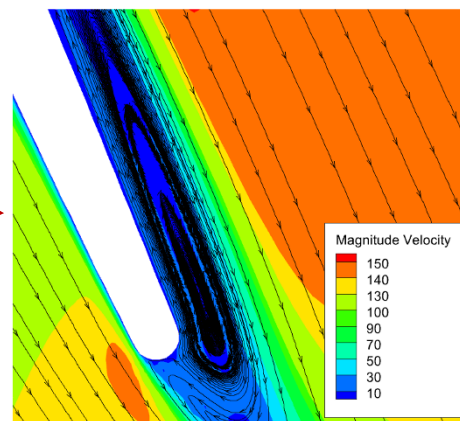
The simulations were performed with all the five models. All the simulations are performed to ensure that the convergence level is below 10^{-5}. A typical residual convergence plot with the LKE model is shown in Figure 3. Fair convergence is achieved after 1000 iterations. First-cell distance in wall-units (Y^+) around the blade is maintained below 1 for most of the blade. Figure 4 presents the Y^+ distribution based on the simulation.

Figure 5 presents the comparison of numerically computed CFD results with experimental results in terms of coefficient of static pressure. As clearly depicted by the plot, all the models predict the flow well on the pressure side of the blade. But in case of the suction side, SA, k-ω SST, realizable k-ε models fail to resolve the flow on the aft portion. This is due to the separation involved, as portrayed by the relatively flat region in the experimental points near the trailing edge. However, both the transition models employed here predict the flow quite well even in the separation region on suction side. Both transition γ-Re_θ and transition k-k_l-ω (Laminar Kinetic Energy) models resolved flow behavior throughout the blade except for a slight difference at the trailing edge. The comparison of isentropic Mach number is presented in Fig. 6. In this case too, all the models provide almost similar results on the suction side. Predictions by the TKE model are slightly closer to the experimental values than the γ-Re_θ transition model.

Now, we describe the detailed flow features as obtained from γ-Re_θ and k-k_l-ω model simulations. Figure 7 presents the velocity streamlines for the γ-Re_θ transition model. The separation bubble on the suction side of the blade is resolved in this case. But it is visible from the streamline plot that the separation bubble thins down as it moves towards the trailing edge. The flow seems to almost reattach as it reaches the trailing edge. Figure 8 presents the streamline plot for the LKE model. The plot clearly illustrates the separation bubble at the aft portion of the blade at the suction side. The flow on the suction side remains separated and an open separation bubble is formed. A zoomed view of this bubble is shown in Fig. 9. The structure of this bubble is very close to that obtained from a high-resolution DNS study by Ranjan *et al.* [26] as shown in Fig. 10.

Figure 8: Velocity Streamlines (LKE)

Figure 9: Zoomed View
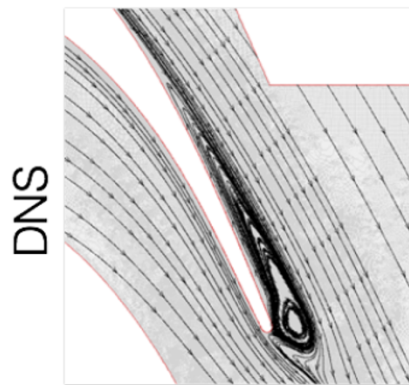
Figure 10: T106A flow separation using high-resolution DNS study (reproduced from Ranjan *et al.* [15])
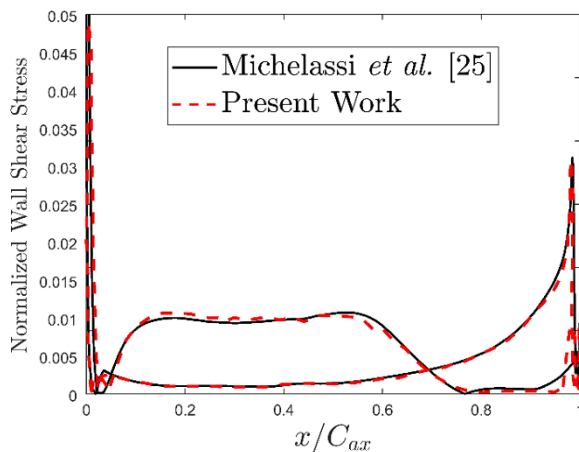
Figure 11: Normalized Wall Shear

The onset of separation can be explored by referring to Figure 5, where the flat portion of the suction side of the C_p plot indicates separation. This separation onset is at around 0.8 C_{ax}. Figure 11 shows the normalized absolute wall-shear stress plot which further confirms this. The absolute wall shear stress starts to tend to zero at the said location. The results are compared with the DNS study by Michelassi *et al.* [25] . An appreciable match is found with the DNS results. The velocity streamlines plot for the laminar kinetic energy model in the present study is in close agreement with the DNS results. Another hybrid RANS-LES simulation [18] also shows similar flow structure.

5. CONCLUSIONS

In the present work, results obtained by RANS simulations of transitional flow past a LPT blade T106A were presented. The present work focused upon predicting the separation and studying the transition over the blade under low Reynolds number and high incidence configuration.

The flow was simulated using 3 commonly used turbulence models (SA, kω-SST, Realizable k-ε). These models were able to predict the flow on the pressure side of the blade quite well but failed to resolve the flow on the suction side, where the separation is involved. On the contrary, the transition models

(laminar kinetic energy (LKE), γ-Re$_θ$) resolved the flow quite well on the same exact grid. An excellent match of the pressure distribution around the blade was found with the experimental results. But in terms of prediction of the flow structure, the LKE model performs better than the γ-Re$_θ$ model. The γ-Re$_θ$ model predicted the separation bubble on the suction side but the location and size were not precise as compared to high resolution DNS studies in the literature. In case of the LKE model, characteristics of the separation bubble were well-predicted. The study suggests that modern transitional models have the potential to be used an engineering design tool for complex LPT flows provided they are extensively validated and verified.

NOMENCLATURE

k	Turbulent kinetic energy	[m^{2}s^{-2}]
ϵ	Dissipation rate	[m^{2}s^{-3}]
γ	Intermittency	
C	Chord length	mm
C_{ax}	Axial chord length	mm
ω	Specific rate of dissipation	[s^{-1}]
β_1	Inlet flow angle	[°]
p_{t1}	Total pressure at inlet	[Pa]
p_1	Static pressure at inlet	[Pa]
p_2	Static pressure at exit	[Pa]

REFERENCES

[1] E. Mazareanu, Commercial airlines worldwide - fuel consumption 2005-2021. statista.com. Retrieved. August 8, 2021 from https://www.statista.com/statistics/655057/fuel-consumption-of-airlines-worldwide/

[2] V. Michelassi, L.-W. Chen, R. Pichler, and R. D. Sandberg, "Compressible Direct Numerical Simulation of Low-Pressure Turbines—Part II: Effect of Inflow Disturbances," Journal of Turbomachinery, vol. 137, no. 7, Jul. 2015.

[3] R. Ranjan, S. M. Deshpande, & R. Narasimha. A High-Resolution Compressible DNS Study of Flow Past a Low-Pressure Gas Turbine Blade. Advances in Computation, Modeling and Control of Transitional and Turbulent Flows, 2015, 291–301. doi:10.1142/9789814635165_0028

[4] R. E. Mayle. Closure to "Discussion of 'The Role of Laminar-Turbulent Transition in Gas Turbine Engines'" (1991, ASME J. Turbomach., 113, pp. 536–537). Journal of Turbomachinery, 113(4), 1991, 537–537. doi:10.1115/1.2929112

[5] H. P. Hodson, and R. J. Howell, Bladerow interactions, transition, and high-lift aerofoils in low-pressure turbines, Annual Review of Fluid Mechanics, 37(1), pp.71–98. 2005. Available at: http://dx.doi.org/10.1146/annurev.fluid.37.061903.175511.

[6] R. D. Stieger, and H. P. Hodson, The Transition Mechanism of Highly-Loaded LP Turbine Blades, Volume 5: Turbo Expo 2003, Parts A and B. 2003. Available at: http://dx.doi.org/10.1115/gt2003-38304.

[7] H. D. Akolekar, Turbulence Model Development & Implementation for Low Pressure Turbines Using a Machine Learning Approach. (Doctoral thesis, University of Melbourne, Australia). (August 2019).

[8] A. Hatman, and T. Wang, A Prediction Model for Separated-Flow Transition. Journal of Turbomachinery, 121(3), 1999, pp.594–602. Available at: http://dx.doi.org/10.1115/1.2841357.

[9] V. Marciniak, R. Kuegeler, and M. Franke, Predicting Transition on Low-Pressure Turbine Profiles. V European conference on computational fluid dynamics ECCOMAS CFD. Vol. 2010, 2010

[10] R. Skoda, R. Schilling, and M. T. Schobeiri, Numerical Simulation of the Transitional and Unsteady Flow through a Low-Pressure Turbine. International Journal of Rotating Machinery, 2007, 1–11. doi:10.1155/2007/10940

[11] P. Stadtmüller, L. Fottner, and A. Fiala, Experimental and Numerical Investigation of Wake-Induced Transition on a Highly Loaded LP Turbine at Low Reynolds Numbers. Proceedings of the ASME Turbo Expo 2000: Power for Land, Sea, and Air. Volume 3: Heat Transfer; Electric Power; Industrial and Cogeneration. Munich, Germany. May 8–11, 2000. V003T01A074. ASME. https://doi.org/10.1115/2000-GT-0269

[12] L. Hilgenfeld, P. Stadtmüller, and L. Fottner, Experimental Investigation of Turbulence Influence of Wake Passing on the Boundary Layer Development of Highly Loaded Turbine Cascade Blades. Flow, Turbulence and Combustion 69, 229 (2002). https://doi.org/10.1023/A:1027351020947

[13] G. Kalitzin, X. Wu, and P.A. Durbin, DNS of fully turbulent flow in a LPT passage. International Journal of Heat and Fluid Flow, 24(4), pp.636–644., 2003. http://dx.doi.org/10.1016/s0142-727x(03)00057-2.

[14] R. Ranjan, S. M. Deshpande, and R. Narasimha, New insights from high-resolution compressible DNS studies on an LPT blade boundary layer. Computers & Fluids, 153, 2017, 49–60. doi:10.1016/j.compfluid.2017.05.004

[15] Y. Zhao, H. D. Akolekar, J. Weatheritt, V. Michelassi, and R. D. Sandberg, RANS turbulence model development using CFD-driven machine learning. Journal of Computational Physics, 411, 2020. 109413. doi:10.1016/j.jcp.2020.109413

[16] R. Ranjan, S. M. Deshpande, and R. Narasimha, A High-Resolution Compressible DNS Study of Flow Past a Low-Pressure Gas Turbine Blade. Advances in Computation, Modeling and Control of Transitional and Turbulent Flows, 2015, 291–301. doi:10.1142/9789814635165_0028

[17] R. Pichler, R. D. Sandberg, V. Michelassi, and R. Bhaskaran, Investigation of the Accuracy of RANS Models to Predict the Flow Through a Low-Pressure Turbine. ASME. J. Turbomach. December 2016; 138(12): 121009. https://doi.org/10.1115/1.4033507

[18] R. Ranjan, S. M. Deshpande, and R. Narasimha, Prediction of separation and transition on a low-pressure turbine blade using a RANS grid, 2020

[19] P. Stadtmuller, Investigation of wake-induced transition on the LP turbine cascade T106A-EIZ. Tech. Rep. 2002

[20] R. D. Sandberg, R. Pichler, and L. Chen, Assessing the sensitivity of turbine cascade flow to inflow disturbances using direct numerical simulation. 13th International Symposium for Unsteady Aerodynamics, Aeroacoustics and Aeroelasticity in Turbomachinery (ISUAAAT), Tokyo, Japan. 10 - 13 Sep 2012.

[21] V. Michelassi, J. Wissink, and W. Rodi, Analysis of DNS and LES of Flow in a Low-Pressure Turbine Cascade with Incoming Wakes and Comparison with Experiments. Flow, Turbulence and Combustion 69, 2002, 295–329. https://doi.org/10.1023/A:1027334303200

[22] G. S. François, About Boussinesq's turbulent viscosity hypothesis: historical remarks and a direct evaluation of its validity, Comptes Rendus Mécanique, Volume 335, Issues 9–10, 2007, Pages 617-627, ISSN 1631-0721, https://doi.org/10.1016/j.crme.2007.08.004.

[23] M. Leschziner, Statistical Turbulence Modelling for Fluid Dynamics - Demystified: an Introductory Text for Graduate Engineering Students. World Scientific. 2015.

[24] ANSYS Fluent User's Guide v 2020 R1

[25] R. D. Sandberg, V. Michelassi, R. Pichler, L. Chen, R. Johnstone, Compressible Direct Numerical Simulation of Low-Pressure Turbines —Part I: Methodology; ASME. J. Turbomach. 2015;137(5):051011 .

[26] R. Ranjan, S. M. Deshpande, and R. Narasimha, A Critical Comparison of RANS, LES, Hybrid LES/RANS and DNS Studies of the Flow Past a Low-Pressure Turbine Blade in a Cascade, 2016.